

AD-A051 736

AIR FORCE GEOPHYSICS LAB HANSCOM AFB MASS  
AN EFFICIENT, ACCURATE NUMERICAL METHOD FOR THE SOLUTION OF A P--ETC(U)  
NOV 77 S Y YEE

F/G 12/1

UNCLASSIFIED

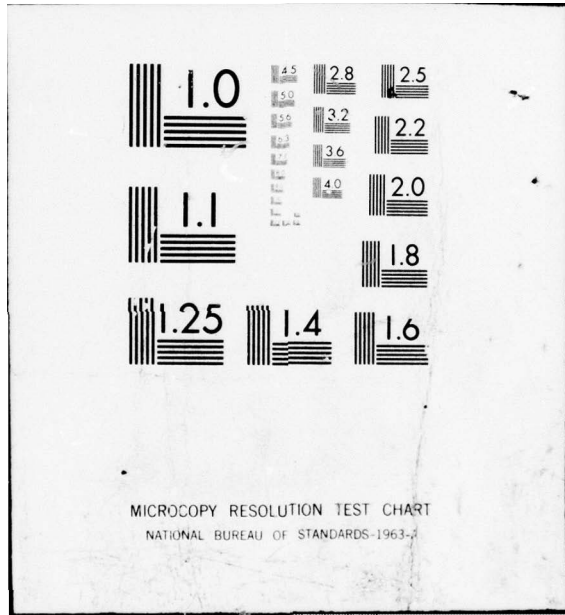
AFGL-TR-77-0246

NL

| OF |  
AD  
A051736



END  
DATE  
FILMED  
4-78  
DDC



MICROCOPY RESOLUTION TEST CHART  
NATIONAL BUREAU OF STANDARDS-1963-A

2

AFGL-TR-77-0246  
ENVIRONMENTAL RESEARCH PAPERS, NO. 612



*Handwritten mark*

AD A051736

# An Efficient, Accurate Numerical Method for the Solution of a Poisson Equation on a Sphere

SAMUEL Y. K. YEE

AD No. \_\_\_\_\_  
DDC FILE COPY

4 November 1977

DDC  
RECEIVED  
MAR 24 1978  
B

Approved for public release; distribution unlimited.

METEOROLOGY DIVISION PROJECT 2310  
AIR FORCE GEOPHYSICS LABORATORY  
HANSCOM AFB, MASSACHUSETTS 01731

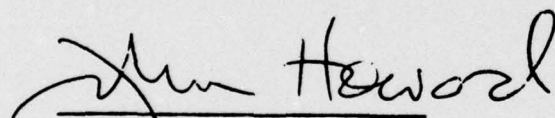
AIR FORCE SYSTEMS COMMAND, USAF



This report has been reviewed by the ESD Information Office (OI) and is releasable to the National Technical Information Service (NTIS).

This technical report has been reviewed and is approved for publication.

FOR THE COMMANDER

  
\_\_\_\_\_  
Chief Scientist

Qualified requestors may obtain additional copies from the Defense Documentation Center. All others should apply to the National Technical Information Service.

14 AFGL-TR-77-0246  
AFGL-ERP-612

Unclassified

SECURITY CLASSIFICATION OF THIS PAGE (When Data Entered)

REPORT DOCUMENTATION PAGE		READ INSTRUCTIONS BEFORE COMPLETING FORM
1. REPORT NUMBER AFGL-TR-77-0246 ✓	2. GOVT ACCESSION NO.	3. RECIPIENT'S CATALOG NUMBER
4. TITLE (and Subtitle) AN EFFICIENT, ACCURATE NUMERICAL METHOD FOR THE SOLUTION OF A POISSON EQUATION ON A SPHERE. ✓	5. TYPE OF REPORT & PERIOD COVERED Scientific-Environmental Research Papers Oct 76-Sep 77	6. PERFORMING ORG. REPORT NUMBER ERP No. 612 ✓
7. AUTHOR(s) Samuel Y. K. Yee	8. CONTRACT OR GRANT NUMBER(s)	
9. PERFORMING ORGANIZATION NAME AND ADDRESS Air Force Geophysics Laboratory (LYD) Hanscom AFB Massachusetts 01731 ✓	10. PROGRAM ELEMENT, PROJECT, TASK AREA & WORK UNIT NUMBERS 61102F 2310G203	J6 2310 17 G2
11. CONTROLLING OFFICE NAME AND ADDRESS Air Force Geophysics Laboratory (LYD) Hanscom AFB Massachusetts 01731	12. REPORT DATE 4 November 1977 ✓	
14. MONITORING AGENCY NAME & ADDRESS (if different from Controlling Office)	13. NUMBER OF PAGES 20	12 21P
	15. SECURITY CLASS. (of this report) Unclassified	
	15a. DECLASSIFICATION/DOWNGRADING SCHEDULE	
16. DISTRIBUTION STATEMENT (of this Report) Approved for public release; distribution unlimited.		
17. DISTRIBUTION STATEMENT (of the abstract entered in Block 20, if different from Report)		
18. SUPPLEMENTARY NOTES		
19. KEY WORDS (Continue on reverse side if necessary and identify by block number) Poisson equation Boundary value problem Shooting method Flexible difference scheme		
20. ABSTRACT (Continue on reverse side if necessary and identify by block number) The need for efficient and accurate methods for the solution of boundary value problems such as Poisson-type equations is well established. In numerical weather prediction where solutions to such equations are required in daily routine operations, it is paramount that the solution procedure be efficient. We have reported earlier an efficient shooting method to meet such a need. The algebraic system resulting from the regular discretization of the Poisson equation on a sphere is, however, numerically unstable. Thus the direct application of this method is accurate only for relatively small systems. → next page		

has been reported

DD FORM 1 JAN 73 1473 EDITION OF 1 NOV 65 IS OBSOLETE

Unclassified  
SECURITY CLASSIFICATION OF THIS PAGE (When Data Entered)

409 578 JOB



Unclassified

SECURITY CLASSIFICATION OF THIS PAGE(When Data Entered)

20. Abstract (Continued)

This limitation has now been successfully removed by two major improvements to the method. The inherent instability of the system due to a spectral radius larger than unity is alleviated by the use of a multiple shooting technique, while the instability due to the convergence of meridians on a sphere is overcome by a specially designed flexible grid. Numerical examples are provided to demonstrate the effectiveness of the improved method.

Unclassified

SECURITY CLASSIFICATION OF THIS PAGE(When Data Entered)

ACCESSION for	
NTIS	White Section <input checked="" type="checkbox"/>
DDC	Buff Section <input type="checkbox"/>
UNANNOUNCED	<input type="checkbox"/>
JUSTIFICATION _____	
BY _____	
DISTRIBUTION/AVAILABILITY CODES	
Dist.	AVAIL. and/or SPECIAL
A	

## Contents

1. INTRODUCTION	5
2. SYNOPSIS OF METHOD	7
3. THE USE OF MULTIPLE SHOOTING	9
4. THE USE OF FLEXIBLE GRID	15
5. CONCLUDING REMARKS	19
REFERENCES	20

## Illustrations

1. Effect of Subdivision, Standard Grid	14
2. Effect of Flexible Grid	18

## Tables

1. Error Norms in the Computed Solution as a Function of $m$ , constant $\Delta\lambda$	14
2. Spatial Increments in $\lambda$ as Function of Latitude for a $64 \times 64$ Grid	16
3. Error Norms in the Computed Solution as a Function of $m$ , variable $\Delta\lambda$	18

## An Efficient, Accurate Numerical Method for the Solution of a Poisson Equation on a Sphere

### 1. INTRODUCTION

The need for efficient and accurate methods for the solution of Poisson-type equations in mathematical physics is well established. Important texts in numerical analysis such as *Matrix Iterative Analysis* (Varga<sup>1</sup>) are not only eloquent testimonies to the magnitude of the problem, but also vivid evidence of the extent of the interest. In the case of numerical weather prediction, where solutions to the Poisson equation are required in daily routine operations, it is paramount that the solution procedure be efficient. In anticipation of the development of global numerical weather prediction models, we developed earlier an efficient shooting algorithm for the solution of a discrete Poisson equation on the surface of a sphere (Yee<sup>2</sup>). This report presents the most recent development in our work along this line.

We seek a numerical solution to the Poisson equation on the surface of a unit sphere,

---

(Received for publication 28 October 1977)

1. Varga, R. S. (1962) *Matrix Iterative Analysis*, Prentice-Hall, Englewood Cliffs, N. J.
2. Yee, S. Y. K. (1976) An efficient method for a finite-difference solution of the Poisson equation on the surface of a sphere, *J. Comput. Phys.* 22:215-228.



$$\left( \frac{1}{\sin \theta} \frac{\partial}{\partial \theta} \sin \theta \frac{\partial}{\partial \theta} + \frac{1}{\sin^2 \theta} \frac{\partial^2}{\partial \lambda^2} \right) u = f(\theta, \lambda) \quad . \quad (1)$$

Here  $0 \leq \theta \leq \pi$  is the colatitude and  $0 \leq \lambda \leq 2\pi$  is the longitude. Discretization of this equation using a five-point centered-difference operator for the Laplacian gives the following  $I \times J$  linear algebraic system

$$a_i \bar{u}_{i-1} - (a_i + b_i) \bar{u}_i + b_i \bar{u}_{i+1} - c_i R \bar{u}_i = \bar{f}_i \quad , \quad 1 \leq i \leq I \quad , \quad (2)$$

where

$$\bar{u}_i = \begin{pmatrix} u_{i,1} \\ \vdots \\ u_{i,j} \\ \vdots \\ u_{i,J} \end{pmatrix} \quad , \quad \bar{f}_i = \begin{pmatrix} f_{i,1} \\ \vdots \\ f_{i,j} \\ \vdots \\ f_{i,J} \end{pmatrix} \quad ,$$

$$R = \begin{pmatrix} 2 & -1 & -1 \\ -1 & & -1 \\ -1 & -1 & 2 \end{pmatrix} \quad ,$$

$$u_{i,j} = u(\theta_i, \lambda_j) \quad ,$$

$$f_{i,j} = f(\theta_i, \lambda_j) \quad ,$$

$$\theta_i = \left( i - \frac{1}{2} \right) \Delta\theta \quad ,$$

$$\lambda_j = j \Delta\lambda \quad ,$$

$$\Delta\theta = \pi/I \quad ,$$

$$\Delta\lambda = 2\pi/J \quad ,$$

$$a_i = \frac{\sin \theta_{i-1/2}}{\Delta\theta^2 \sin \theta_i} \quad ,$$

$$b_i = \frac{\sin \theta_{i+1/2}}{\Delta\theta^2 \sin \theta_i} \quad ,$$

$$c_i = \frac{1}{(\Delta\lambda)^2 \sin^2 \theta_i} \quad .$$

Here we have excluded from consideration the coordinate singularities at the poles by adopting the spherical grid system proposed by Merilees.<sup>3</sup> We have also gridded the surface of the sphere with I grid points along a meridian and J grid points along a latitude. Note that a solution for Eq. (2) exists only if its right-hand side satisfies the compatibility condition

$$\sum_{i=1}^I \sin \theta_i \sum_{j=1}^J f_{i,j} = 0 \quad . \quad (3)$$

Even then, since the coefficient matrix of Eq. (2) is singular, with its rank one less than its order ( $a_1 = b_1 = 0$ ), the solution can be determined only to within an additive constant. This is consistent with the fact that, for the lack of lateral boundaries on a sphere, a solution to Eq. (1) can only be determined to within an additive constant.

Equation (2), however, is prone to numerical instability. First, the coefficient matrix of Eq. (2) has a spectral radius that is larger than unity. Furthermore, because of the convergence of meridians on a sphere, the condition number of the system increases rapidly with increasing spatial resolution of the computational grid. These instability properties severely limit the usefulness of the simple shooting method reported earlier to relatively coarse grid resolutions. For larger systems resulting from finer resolutions, because of the inherent numerical instability mentioned above, direct application of this method will give inaccurate results. It is the purpose of this report to demonstrate that this numerical instability problem can be remedied by a two-pronged approach. The instability due to a spectral radius larger than unity is alleviated by the use of a multiple shooting technique, while that due to a large condition number is overcome by the use of a flexible grid.

## 2. SYNOPSIS OF METHOD

To view the shooting method described here from a proper perspective, we shall first review in this section a classical method for the solution of differential equations. It will then be easy to see that this method is indeed no more than the implementation, in the discrete domain, of a solution method in differential equations. The classical approach for the solution of a differential equation separates

---

3. Merilees, P. E. (1973) Pseudospectral approximation applied to the shallow water equations, Atmosphere 11:13-20.

the complete solution into two parts, a particular part and a homogeneous part. For example (Berg and McGregor<sup>4</sup>), for the boundary value problem

$$\begin{aligned} \nabla^2 u &= f \quad \text{in } R \quad , \\ u &= u^* \quad \text{on } B \quad , \end{aligned} \tag{4}$$

it is often easy to find a particular solution  $u_P$  which satisfies only the differential equation

$$\nabla^2 u_P = f \quad .$$

Continuity requirements on the boundary then give us  $u_P^*$  values of  $u_P$  on the boundary. We solve next for  $u_H$  in the homogeneous system

$$\begin{aligned} \nabla^2 u_H &= 0 \quad \text{in } R \quad , \\ u_H &= u^* - u_P^* \quad \text{on } B \quad . \end{aligned} \tag{5}$$

The complete solution for Eq. (4) is then given by

$$u = u_P + u_H \quad .$$

Equation (2) is a discrete form of an inhomogeneous two-dimensional linear elliptic equation applied in a closed region with no external boundary. It may be looked upon as a discrete boundary value problem in the sense that, although subject to no explicit external boundary constraints, it must satisfy the global constraint Eq. (3). We, therefore, propose to solve Eq. (2) in two steps. First, we construct a particular solution which, except at certain preselected grid latitudes  $\theta_1$ , satisfies Eq. (2). One way of constructing such a particular solution for Eq. (2) is to assume arbitrary values for the components of  $\vec{u}_1$ , at  $\theta_1$ . We may then compute by a marching procedure a solution of the equation for the rest of the region. At  $\theta_1$ , the forcing function  $\vec{f}_1^*$  computed from the particular solution will be different, in general, from the given  $\vec{f}_1$ . The particular solution, therefore, does not satisfy Eq. (2) at  $\theta_1$ . We next "correct" these discrepancies by adding to the particular solution the homogeneous solution to Eq. (2). Since the homogeneous equation has only J non-zero components ( $\vec{f}_1 - \vec{f}_1^*$ ) in its forcing function, it can be solved with less computing effort than that required for the inhomogeneous equation.

4. Berg, P. W., and McGregor, J. L. (1966) Elementary Partial Differential Equations, Holden-Day, San Francisco, CA.



Instead of computing the homogeneous solution for the entire region, the shooting method computes first the complete solution at selected grid latitudes (the "missing initial conditions"). The complete solution for the remainder of the grid is then obtained by a marching procedure (shooting). The key idea here is that, by the use of shooting, we avoid most of the transform operations needed to compute the homogeneous solution for the entire region.

Although the idea here is to avoid the need of calculating the entire homogeneous solution, looking at the shooting method as just a way of implementing a classical method in differential equation is useful because it provides us with the insight to compute easily the "missing initial conditions" through the judicious use of Fourier transforms. This is especially desirable in the case of multiple shooting where we have to seek the "missing initial conditions" at a number of grid latitudes. We emphasize here that the construction of a particular solution for Eq. (2) is accomplished simply by marching in the two-dimensional physical domain. Details of computing the "missing initial conditions" are described in Section 3 in connection with the multiple shooting algorithm.

### 3. THE USE OF MULTIPLE SHOOTING

We mentioned in Section 1 that the shooting method is inaccurate for the numerical solution of Eq. (2) when I and J are large. This difficulty can be alleviated somewhat by the use of a multiple shooting technique, a straightforward extension of the approach described in Section 2. With this approach, a sphere is divided into subregions by pairs of internal computational boundaries. A particular solution is then constructed for each of the subregions. Again these solutions satisfy Eq. (2) except at certain prespecified  $\theta_i$ . They, therefore, constitute a particular solution for the sphere as a whole. To this particular solution, we now add the homogeneous solution of Eq. (2) to form the complete solution. This time, the forcing function of the homogeneous equation has, however, a number of pairs of nonzero component vectors due to the arbitrarily picked internal computational boundary conditions.

For pedagogic purposes, we shall detail here a method for obtaining a homogeneous solution to Eq. (2). The method makes use of similarity transforms to reduce first the block-tridiagonal system Eq. (2) to a system of tridiagonal systems. The homogeneous solutions to these reduced systems are then computed by an efficient Gaussian elimination algorithm (Varga<sup>1</sup>). The motivation of such an approach has been discussed earlier (Yee<sup>2</sup>).

If we perform a discrete Fourier transform on  $\vec{u}_i$  and  $\vec{f}_i$  and let

$$\vec{w}_i = P^{-1} \vec{u}_i, \quad \vec{g}_i = P^{-1} \vec{f}_i \quad (6)$$



we may write Eq. (2) in a space-Fourier domain for  $1 \leq i \leq I$ ,

$$a_i \vec{w}_{i-1} - (a_i + b_i) \vec{w}_i + b_i \vec{w}_{i+1} - c_i D \vec{w}_i = \vec{g}_i, \quad (7)$$

where

$$\vec{w}_i = \begin{pmatrix} w_{i,1} \\ \vdots \\ w_{i,k} \\ \vdots \\ w_{i,K} \end{pmatrix}, \quad \vec{g}_i = \begin{pmatrix} g_{i,1} \\ \vdots \\ g_{i,k} \\ \vdots \\ g_{i,K} \end{pmatrix}$$

and  $D = P^{-1} R P$ ,  $K = J$ . Here the diagonal elements of the diagonal matrix  $D$  are the eigenvalues  $d_{k,k}$  of  $R$ , and  $P$  is a  $J \times J$  orthogonal matrix whose columns are the normalized eigenvectors associated with  $d_{k,k}$ , that is,

$$d_{k,k} = 2(1 - \cos \lambda_k), \quad 1 \leq k \leq K, \\ P_{j,k} = \left( \frac{2}{J} \right)^{1/2} \begin{pmatrix} \cos j\lambda_k, & 1 \leq k \leq (K/2) - 1, \\ (\cos j\lambda_k)/2^{1/2}, & k = K/2, \\ -\sin j\lambda_k, & (K/2) + 1 \leq k \leq K - 1, \\ 1/2^{1/2}, & k = K, \end{pmatrix}, \quad 1 \leq j \leq J. \quad (8)$$

Grouping  $w_{i,k}$  by components and defining

$$\vec{w}_k = \begin{pmatrix} w_{1,k} \\ \vdots \\ w_{i,k} \\ \vdots \\ w_{I,k} \end{pmatrix}, \quad \vec{g}_k = \begin{pmatrix} g_{1,k} \\ \vdots \\ g_{i,k} \\ \vdots \\ g_{I,k} \end{pmatrix},$$



$$\Delta \vec{g}_k \equiv \vec{g}_k - \vec{g}_k^i = \begin{pmatrix} 0 \\ \vdots \\ 0 \\ b_\ell \Delta w'_{\ell+1, k} \\ a_{\ell+1} \Delta w'_{\ell, k} \\ 0 \\ \vdots \\ 0 \\ b_{3\ell} \Delta w'_{3\ell+1, k} \\ a_{3\ell+1} \Delta w'_{3\ell, k} \\ 0 \\ \vdots \\ 0 \end{pmatrix}, \quad \ell \equiv I/4. \quad (12)$$

Here  $\Delta w'_{i, k}$  is the discrepancy of the  $k$ th component, at  $\theta_i$ , of the two marching solutions from opposite boundaries of a subregion. Thus if  $\vec{S}_k$  is a solution to the homogeneous system for Eq. (9),

$$T_k \vec{S}_k = \Delta \vec{g}_k, \quad (13)$$

then the complete solution to Eq. (9) is

$$\vec{w}_k = \vec{w}'_k + \vec{S}_k. \quad (14)$$

Once  $\vec{w}_k$  is available for all  $k$ ,  $\vec{u}_i$  may then be computed from the inverse transform to Eq. (6),

$$\vec{u}_i = P \vec{w}_i. \quad (15)$$

At this point, it is appropriate to point out that the derivations detailed here serve only to demonstrate that in the case of multiple shooting, the "missing initial conditions" can easily be obtained by solving tridiagonal systems such as Eq. (13). As mentioned earlier in Section 2, for reasons of computational

efficiency, we use neither Eq. (12) to yield  $\Delta \vec{g}_k$ , nor Eq. (15) to obtain  $\vec{u}_1$ . In practice,  $\vec{u}_1$  may be computed by the use of a much more efficient shooting algorithm (Yee<sup>2</sup>).

Test computations, using the multiple shooting technique, have been made for system (2) for various  $n$ , the number of shooting subregions, and for several values of  $I$  and  $J$ . The design of the numerical tests is the same as that reported in Yee.<sup>2</sup> Namely, we create a set of true solution  $v_{i,j}$  for Eq. (2) by computing  $f_{i,j}$  from

$$f_{i,j} = a_i v_{i-1,j} - (a_i + b_i + 2c_i) v_{i,j} + b_i v_{i+1,j} + c_i (v_{i,j-1} + v_{i,j+1}) .$$

Here values for  $v_{i,j}$  are obtained from a random number generator and have been subjected to the constraint  $\sum_i \sum_j v_{i,j} = 0$  so that  $f_{i,j}$  satisfies the compatibility condition Eq. (3). With the forcing function  $f_{i,j}$  computed in this manner, a normalized error norm defined by

$$\|E\|_2 = \|u - v\|_2 / \|v\|_2$$

may then be considered as a measure of the accuracy of the numerical procedure. The number of digits of accuracy in  $u$  is then given by

$$Z = -\log_{10} \|E\|_2 .$$

Table 1 gives sample results for a  $64 \times 64$  grid in terms of  $Z$ ,  $\|E\|_2$  and  $|E(\text{Max})|$ , the magnitude of the maximum error over the entire computational region. Here  $n$  is the number of subregions into which the surface of the sphere is divided and  $m$  is the number of grid latitudes within each subregion. Thus for  $n = 1$ ,  $m = 32$ , for example, the entire surface of the sphere is treated as one region, and shooting is conducted from both poles over a shooting range of 32 grid latitudes toward the equator. Inspection of Table 1 gives us the impression that for the case of a  $64 \times 64$  sphere, this method is useful only when the sphere is divided into a relatively large number of latitude bands. For example, for the case of  $n = 4$ , we have  $Z = 1.6$ , that is, less than two-digit accuracy in our results. Careful study of the distribution of the error fields suggests, however, that due to the convergence of meridian on a sphere, the largest local errors invariably occur in the computational subregions containing the polar caps. Furthermore, these errors are considerably larger in magnitude than those in other subregions. This phenomenon is well borne out by Figure 1 which depicts typical error distributions as a function of  $\theta_i$  for the cases of  $n = 4$  and  $n = 8$ . We see from this figure that, except for the subregions containing the polar caps, we have for the



Table 1. Error Norms in the Computed Solution\* as a Function of m

m	n	Z	$\ E\ _2$	$ E(\text{Max}) $
2	16	9.6	$2.2 \times 10^{-10}$	$1.0 \times 10^{-9}$
4	8	6.4	$3.6 \times 10^{-7}$	$2.8 \times 10^{-6}$
8	4	1.6	$2.3 \times 10^{-2}$	$2.0 \times 10^{-1}$
16	2	-6.2	$1.7 \times 10^6$	$2.4 \times 10^7$
32	1	-21.4	$2.2 \times 10^{21}$	$3.4 \times 10^{22}$

Z Number of digits of accuracy in computed solution u.

\* For a  $64 \times 64$  grid with constant  $\Delta\lambda$ .

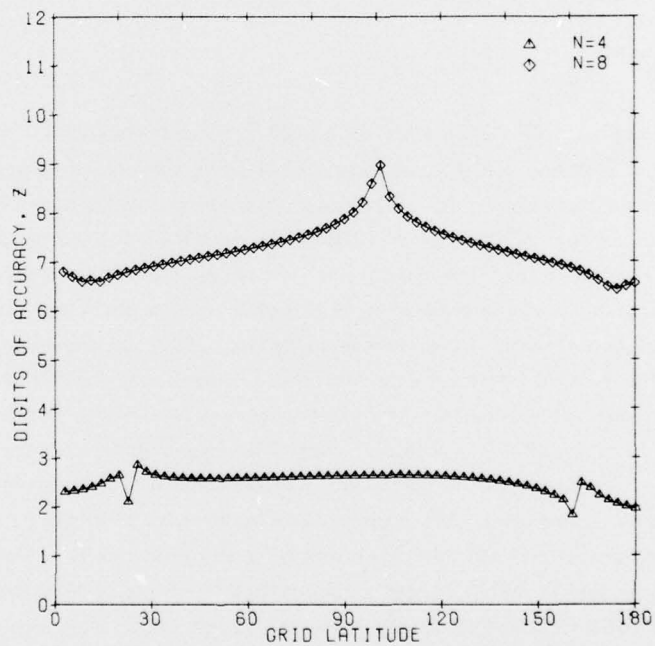


Figure 1. Effect of Subdivision, Standard Grid

case of  $n = 4$  more than two-digit accuracy in our results. Comparison of the error distributions of these two cases also suggests that increasing the number of subregions is not an effective way to reduce the deleterious effect due to the convergence of meridians. Other more effective means must be sought if we want to use a grid with high resolution.

#### 4. THE USE OF FLEXIBLE GRID

It is easy to see that the numerical instability inherent in the solution of Eq. (2) is due in part to the convergence of meridians on a sphere. From the definition of  $c_i$  in Eq. (2),

$$c_i = \frac{1}{\Delta\lambda^2 \sin^2 \theta_i}$$

we see that  $c_i \rightarrow \infty$  as  $\sin^2 \theta_i \rightarrow 0$ . Thus if  $\Delta\lambda$  is not a function of  $\theta_i$ , increased resolution in  $\Delta\theta$  tends to destabilize the solution through the rapid increase of the condition number of the coefficient matrix of Eq. (2). We shall demonstrate in this section how this difficulty can be circumvented by the use of a flexible finite-difference scheme.

Consider the following finite-difference approximation to the second term of Eq. (1),

$$\left( \frac{1}{\sin^2 \theta} \frac{\partial^2 u}{\partial \lambda^2} \right)_{i,j} \simeq \frac{1}{\beta_i^2 \sin^2 \theta_i} (u_{i,j-\beta_i} - 2u_{i,j} + u_{i,j+\beta_i}) + \frac{1}{\sin^2 \theta_i} O(\beta_i^2) \quad (16)$$

where  $\beta_i = \Delta\lambda_i$ . From the numerical stability point of view, it is desirable to keep the value of  $(\beta_i \sin \theta_i)^2$  from approaching zero. The simplest way of achieving this is of course to set  $\beta_i = 1/\sin \theta_i$ . This is, however, impractical because the points  $(i, j-\beta_i)$ ,  $(i, j+\beta_i)$  in Eq. (16) will not in general coincide with the regular grid points. To insure that the points  $(i, j\pm\beta_i)$  coincide with the grid points, we must have  $\beta_i$  take on only multiple values of  $\Delta\lambda$ , that is,

$$\beta_i = h_i \Delta\lambda$$

where  $h_i$  are positive integers. Since considerations of maintaining a uniform increment in actual distance on a sphere give us

$$h_i^1 = \frac{J}{I} \frac{1}{\sin \theta_i} ,$$

we therefore simply pick as  $h_i$  the integer values which are closest to  $h_i^1$ . Under these restrictions, we may now write Eq. (16) as

$$\left( \frac{1}{\sin^2 \theta} \frac{\partial^2 u}{\partial \lambda^2} \right)_{i,j} \approx \frac{1}{h_i^2 \Delta \lambda^2 \sin^2 \theta_i} (u_{i,j-h_i} - 2u_{i,j} + u_{i,j+h_i}) + \frac{1}{\sin^2 \theta_i} O(h_i^2 \Delta \lambda^2) . \quad (17)$$

Table 2 gives the values of  $h_i$  determined in this manner for the case of a  $64 \times 64$  grid. Thus, for example, for  $i = 1$ , we have  $h_i = h_{64} = 16$ , indicating that at the grid latitudes next to the poles, our spatial increments in  $\lambda$  are taken over a distance of  $16 \Delta \lambda$ . In cases where  $I$  is very large, precaution should be taken to insure that the values of  $h_i$  near the poles are small compared to  $J$ .

Table 2. Spatial Increments in  $\lambda$  as Function of Latitude for a  $64 \times 64$  Grid

$i$	$h_i, h_{65-i}$ (unit: $\Delta \lambda$ )
1	16
2	14
3	8
4	6
5	5
6	4
7, 8	3
9, ..., 15	2
16, ..., 32	1

With the use of this differencing scheme, Eq. (2) becomes

$$a_i \bar{u}_{i-1} - (a_i + b_i) \bar{u}_i + b_i \bar{u}_{i+1} - \frac{c_i}{h_i} R_i \bar{u}_i = \bar{F}_i \quad (18)$$

where  $R_i$  are band-tridiagonal  $J \times J$  matrices with their nonzero off-diagonal elements separated from their diagonal elements by  $h_i$  zeros. The element  $r_{t,j}$  of  $R_i$  are given by

$$\begin{aligned}
 r_{t,j} &= 2 \quad , \quad t = j \quad , \quad 1 \leq j \leq J \quad ; \\
 &= -1 \quad , \quad \left( \begin{array}{l} t = j - h_i + J \quad , \quad 1 \leq j \leq h_i \\ t = j \pm h_i \quad \quad , \quad h_i < j < (J - h_i) \\ t = j + h_i - J \quad , \quad (J - h_i + 1) \leq j \leq J \end{array} \right) \quad ; \\
 &= 0 \quad , \quad \text{otherwise.}
 \end{aligned}$$

Note that when  $h_i = 1$ ,  $R_i$  become the matrix  $R$  in Eq. (2). Furthermore, just as  $R$  is orthogonally similar to a real diagonal matrix  $D$ ,  $R_i$  are orthogonally similar to real diagonal matrices  $D_i$ ,

$$D_i = P^{-1} R_i P \quad .$$

Here the elements of  $P$  are given in Eq. (8) and the diagonal elements of  $D_i$  are the eigenvalues  $d_{i,k}$  of  $R_i$ , that is, for a given  $h_i$ ,

$$d_{i,k} = 2(1 - \cos h_i \lambda_k) \quad , \quad 1 \leq k \leq K \quad .$$

Thus with the exception that  $R_i$  are now latitude dependent and we must compute the eigenvalues  $d_{i,k}$  for different  $h_i$ , Eq. (18) may be solved in exactly the same manner Eq. (2) is solved.

Table 3 tabulates sample results when Eq. (18) instead of Eq. (2) is used as the finite-difference analog of Eq. (1). Again the results are for a  $64 \times 64$  grid and the accuracy of the results is measured in terms of error norms. For example, for the case of  $n = 4$ , we now have  $Z = 9.9$ , almost 10-digit accuracy in our numerical results. Comparison of Tables 1 and 3 clearly shows that Eq. (18) is numerically far more stable than Eq. (2). Note that for a given grid resolution, we may choose from tables such as these values of  $n$  to suit our needs, depending on the desired accuracy in our results and the number of digits of accuracy carried by the computer. (Our CDC 6600 carries roughly 15 digits.)

A typical error distribution as a function of latitude for the results of Eq. (18) is given in Figure 2 for a case of  $n = 4$ . Also plotted in Figure 2 is the error curve for the case of  $n = 4$  from Figure 1. Comparison of these two curves clearly demonstrates that the difficulty we had with the use of Eq. (2) has now disappeared.



Table 3. Error Norms in the Computed Solution\* as a Function of m

m	n	Z	$\ E\ _2$	$ E(\text{Max}) $
2	16	11.0	$9.4 \times 10^{-12}$	$1.1 \times 10^{-11}$
4	8	11.0	$9.8 \times 10^{-12}$	$2.6 \times 10^{-11}$
8	4	9.9	$1.3 \times 10^{-10}$	$1.5 \times 10^{-9}$
16	2	6.5	$3.3 \times 10^{-7}$	$5.0 \times 10^{-6}$
32	1	2.2	$6.3 \times 10^{-3}$	$7.0 \times 10^{-2}$

Z Number of digits of accuracy in computed solution u.

\* For a  $64 \times 64$  grid with flexible finite-differencing in  $\lambda$ .

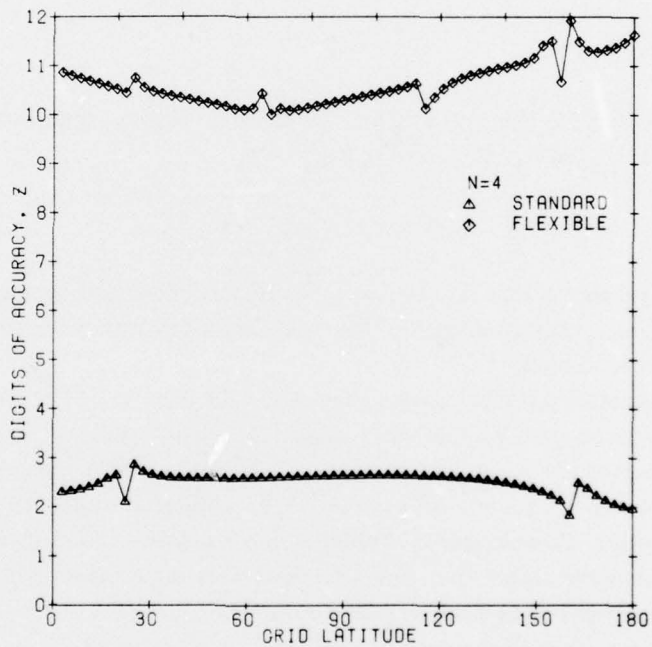


Figure 2. Effect of Flexible Grid

## 5. CONCLUDING REMARKS

The following observations are given as concluding remarks for the work reported here:

(1) The flexible finite-difference scheme described in Section 4 is valuable not only as a means of stabilizing the finite-difference shooting solution for a Poisson equation on a sphere, but it is valuable also for the finite-difference formulation of initial value problems on a sphere, because it enables us to relax the severe restriction on the time increments near the poles in our time integrations. The savings in computer time resulting from this can be substantial.

(2) Other than asserting that it is efficient, we have not discussed here the computational efficiency of this method in relation to other direct methods. That this method is more efficient than many other known methods has been demonstrated in an earlier report (Yee<sup>2</sup>).

(3) As a finite-difference analog to Eq. (1), the truncation error term is larger in Eq. (18) than in Eq. (2) by a factor of  $1/\sin^2 \theta_i$ . Equation (18) is thus less desirable than Eq. (2) from this point of view. This argument in favor of Eq. (2) is lessened somewhat if we recall that other sources of error in  $u$  (observational, round-off) are all inevitably influenced by the same factor  $1/\sin^2 \theta_i$ .

(4) Since the net effect of the flexible grid is to remove the effect of the convergence of meridians on a sphere, the results in Section 4 indirectly indicate that the multiple shooting technique, without incorporating the flexible grid, is a viable tool for solving the Poisson equation in geometries such as rectangles and channels.

(5) Since Fourier transforms are now used only at a few selected grid latitudes, we may, if the situation warrants, elect not to use fast Fourier transform for increased efficiency. This will remove the severe restriction on  $J$ ,  $J = 2^k$ , where  $k$  is a positive integer.

## References

1. Varga, R. S. (1962) Matrix Iterative Analysis, Prentice-Hall, Englewood Cliffs, N. J.
2. Yee, S. Y. K. (1976) An efficient method for a finite-difference solution of the Poisson equation on the surface of a sphere, J. Comput. Phys. 22:215-228.
3. Merilees, P. E. (1973) Pseudospectral approximation applied to the shallow water equations, Atmosphere 11:13-20.
4. Berg, P. W., and McGregor, J. L. (1966) Elementary Partial Differential Equations, Holden-Day, San Francisco, CA.
5. Fox, L. (1957) The Numerical Solution of Two-Point Boundary Problems in Ordinary Differential Equations, Oxford University Press, Fair Lawn, N. J.

78